Dielectric confinement effect in ZnO quantum dots embedded in amorphous SiO_2 matrix

2007 J. Phys. D: Appl. Phys. 40 6071

(http://iopscience.iop.org/0022-3727/40/19/046)

IOP Publishing Journal of Physics D: Applied Physics
J. Phys. D: Appl. Phys. **40** (2007) 6071–6075 doi:10.1088/0022-3727/40/19/046

Dielectric confinement effect in ZnO quantum dots embedded in amorphous SiO_2 matrix

Yu-Yun Peng[1], Tsung-Eong Hsieh[1,3] and Chia-Hung Hsu[2]

[1] Department of Materials Science and Engineering, National Chiao-Tung University, 1001 Ta-Hsueh Road, Hsinchu, Taiwan 300, Republic of China
[2] Research Division, National Synchrotron Radiation Research Center, Hsinchu, Taiwan 300, Republic of China

E-mail: pyy.mse90g@nctu.edu.tw, tehsieh@cc.nctu.edu.tw and chsu@nsrrc.org.tw

Received 21 June 2007
Published 21 September 2007
Online at stacks.iop.org/JPhysD/40/6071

Abstract
The dielectric confinement effect on the blue shift $\Delta E_g(a)$ of the ZnO quantum dots (QDs) embedded in the SiO_2 matrix is evaluated by applying a multi-shell two-electron system model. The experimental measurement and the calculations of various dielectric structures indicate that the composite matrix structure provides a better estimation of the blue shift of the ZnO QDs–SiO_2 system than the multi-shell structure. The proportionality factor x defined in this work exhibits a dependence of the dielectric confinement energy on the specific dimension ratio (the b/a ratio) and the dielectric constant ε_{matrix} of the outer matrix. The result of the calculation also shows the limit of the two-electron system in estimating the ground-state energy of samples with high dot density. However, the correlation shows the existence of the strong dielectric confinement effect in ZnO QDs–SiO_2 thin films and allows a better understanding of the semiconductor QDs–dielectric systems.

1. Introduction

Research on semiconductor quantum dots (QDs) coated with or embedded in various dielectric materials has attracted much attention in recent years. The unique characteristics of such nanostructures are affected not only by the quantum confinement [1] resulting from the nanoscale dimension but also by the dielectric confinement on the electron energies [2–7] and the polarization effect at the unstable surface of QD [8–10]. Previous studies reported that the dielectric environment could effectively change the optical [11–13] and transport [14–17] properties of semiconductor QDs. Many techniques have also been proposed to build a nanostructured semiconductor with a low dielectric-constant matrix into a single-electron device and deliver specific luminescence [12, 13] and single-electron tunnelling [1, 15, 16] properties. Besides distinct optical and electrical properties, a single-electron device enables the integration in a bioenvironment with extremely low power consumption and small current operation, which is quite significant in the application to biotechnology.

The realization of semiconductor QD/dielectric systems in functional devices requires an in-depth understanding of the dielectric effect. The theory of the interaction of the attractive electron–hole Coulomb force and the effect of surface dielectric polarization on semiconductor QDs was introduced in the early 1980s [18, 19]. Surface polarization is induced when charge accumulation in a QD encounters a dielectric mismatch at the QD/matrix interface. Such a polarization effect can lead to a great influence on the confined electron states [20–23], as a result of the creation of extra energies by a single electron interacting with its induced polarization. Further, two (or more) electrons in a QD will interact with the induced polarization created by each other and result in more extra energies. Therefore, the extent of the dielectric confinement is determined by the magnitude of the surface polarization. Consequently, a QD embedded in a glass matrix or liquid solution generally produces stronger confinement than a QD epitaxially grown, due to the substantial

[3] Author to whom any correspondence should be addressed.

Table 1. The variations of the optical bandgaps E_g and the corresponding parameters of ZnO QDs–SiO_2 thin films. The radius a of ZnO QDs was obtained by the histogram with a Gaussian curve fitting and the b/a ratio is the specific dimension ratio. In ZnO QD–SiO_2 thin films, b is the distance from a dot centre to the surface of the neighbouring dot. With the ZnO volume ratio obtained by the x-ray reflectivity measurement, the b/a ratio could be calculated by assuming the randomly distributed QDs in a closest-packing arrangement. The dielectric constant ε_{matrix} was estimated by the Maxwell-Garnett approximation [32].

a (nm)	E_g (eV)	V_{ZnO} (%)	b/a	ε_{matrix}
1.76	3.77 ± 0.04	13.86	2.865	4.376
1.90	3.65 ± 0.03	19.55	2.446	4.583
2.09	3.57 ± 0.05	22.75	2.276	4.703
2.52	3.44 ± 0.04	38.95	1.740	5.345
2.78	3.39 ± 0.04	43.56	1.638	5.540
3.09	3.31 ± 0.03	57.26	1.409	6.155
3.27	3.28 ± 0.04	77.36	1.178	7.168

difference in the dielectric constant and the higher barrier potential.

The effects of the dielectric environment on various semiconductor QDs such as Si, InAs, InP and CdSe have been studied extensively [2–9]. The influence of the dielectric mismatch on the confinement energy of a QD has also been discussed based on the framework of the effective-mass approximation (EMA). This work investigates the dielectric confinement behaviour of a ZnO QD in the amorphous SiO_2 matrix. The *dielectric confinement energy* produced by the polarization effect is calculated by applying a multi-shell two-electron system model. Three dielectric structures are considered in the calculation and all exhibit similar confinement effects on a ZnO QD. In addition to the strong influence of the amorphous SiO_2 dielectric on the optical bandgap E_g of ZnO QDs/SiO_2 nanocomposite films, the results also illustrate the dependence of the dielectric confinement energy on the specific dimension ratio (b/a ratio) and the dielectric constant of the matrix ε_{matrix}.

2. Experiment

ZnO QDs-SiO_2 nanocomposite thin films were prepared by the target-attached sputtering method without substrate heating and post annealing [24, 25]. By changing the sputtering power and the Ar ambient pressure, the thin-film samples containing ZnO QDs with different dot radii and densities could be prepared. The microstructure was characterized by transmission electron microscopy ((TEM), Philips TECNAI 20 FEG Type). The ZnO volume ratios were calculated via the measurement of x-ray reflectivity performed in a Huber four-circle x-ray diffractometer operating at 50 kV and 200 mA with Cu-K_α radiation. The dot radius and volume ratio of each specimen are listed in table 1. Figure 1 shows several TEM images of the ZnO QDs-SiO_2 nanocomposite thin films with different dot radii. It was found that ZnO formed nanoscale crystalline particles embedded in the amorphous SiO_2 matrix [24, 25]. TEM characterization revealed that the ZnO QDs with a small dot radius were completely surrounded by the amorphous SiO_2 matrix and well separated from each another. In contrast, the coalescence of neighbouring QDs occurred in samples with a large dot radius and a high dot density, and the crystallinity of ZnO QDs also increased.

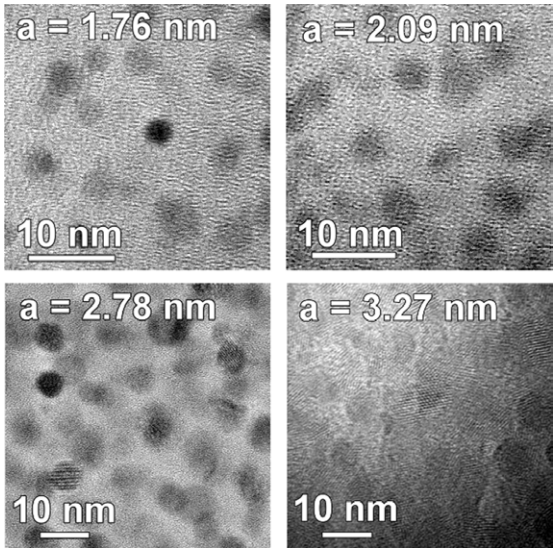

Figure 1. TEM images of the ZnO QDs–SiO_2 nanocomposite films with different dot radii a. The increase in ZnO crystallinity can be observed in the samples with a high dot density.

The optical bandgap E_g of nanocomposite films was determined via the absorption spectra obtained by a UV-visible spectrometer (SHIMADZU UV-1601PC) in the wavelength ranging from 250 to 800 nm. The variation of the E_g with the dot radius is listed in table 1. It is found that E_g increases from 3.28 to 3.77 eV with the decrease in the dot radius from 3.27 to 1.76 nm. The blue shift implies a stronger confinement effect than those of ZnO QDs embedded in air, water [26] and other dielectrics [27].

3. Results and discussion

3.1. Multi-shell two-electron system model

In order to demonstrate the influence of numerous dielectric interfaces on the dielectric confinement, a multi-shell two-electron system model was derived to evaluate the confinement effect in ZnO QDs-SiO_2 nanocomposite films. The multi-shell two-electron system model describes the two-electron ground-state energy of a spherical QD surrounded by periodic dielectric shell layers as illustrated in figure 2(a). The model contains a centred QD with a radius of a and n surrounding shell layers. Overall, there are n interfaces in total, from the dot centre to the outermost dielectric. The thickness of the kth shell layer is denoted as $b-a$ for k = odd and $2a$ for k = even. ε_{k+1} is the static dielectric constant of the kth shell.

When two electrons are put into the centred QD surrounded by a dielectric material, there arise three energy terms: the self-polarization energy $\Delta E_s(a)$, the direct Coulomb energy $\Delta E_c(a)$ and the induced polarization energy $\Delta E_p(a)$. The electrostatic interactions in the multi-shell two-electron system model can be solved by using the standard method [28] as well as that in the previous works presented by Babić *et al* [3] and Iwamatsu *et al* [4]. The self-polarization energy $\Delta E_s(a)$ is

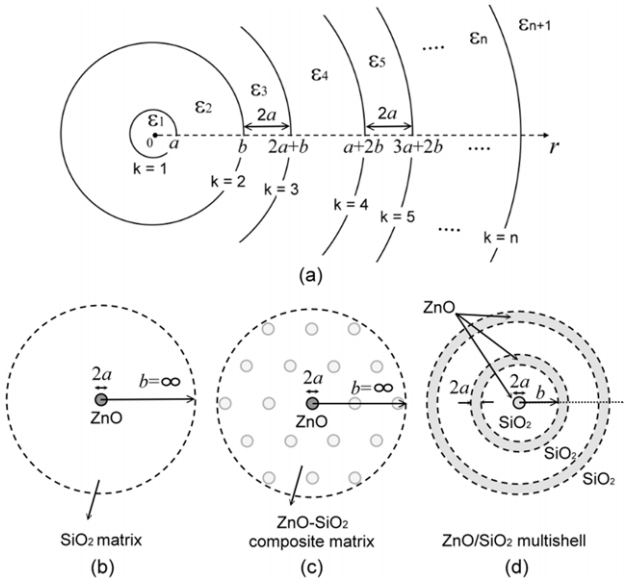

Figure 2. (*a*) The schematic illustration of the multi-shell two-electron system model with n dielectric interfaces. (*b*), (*c*) and (*d*) are the three dielectric structures considered in the calculations: (*b*) structure 1, a single ZnO QD in the SiO_2 matrix, (*c*) structure 2 (*composite matrix structure*), a single ZnO QD within the ZnO–SiO_2 composite matrix and (*d*) structure 3 (*multi-shell structure*), approximately the outer dielectric environment as a multi-shell structure with periodic dielectric shell layers along the closest-packing direction.

formed when an electron inside the centred QD interacts with the polarization potential created itself and can be expressed as

$$\Delta E_s(a) = \frac{e^2}{8\pi\varepsilon_o\varepsilon_1 a} 2\pi^2 \sum_{l=0}^{\infty} a^{2l+1} A_l \int_0^1 j_o^2(\pi x) x^{2l+2}\,\mathrm{d}x \quad (1)$$

with the coefficient A_l given by

$$A_l = (l+1)\left\{ \sum_{\substack{k>0\\ k=\text{odd}}}^{n} \frac{1}{a^{2l+1}} \frac{S_k}{[1+((k-1)/2)(1+(b/a))]^{(2l+1)}} + \sum_{\substack{k>0\\ k=\text{even}}}^{n} \frac{1}{a^{2l+1}} \frac{S_k}{[(b/a)+((k-2)/2)(1+(b/a))]^{(2l+1)}} \right\} \quad (2)$$

$$S_k = \frac{\varepsilon_k - \varepsilon_{k+1}}{\varepsilon_{k+1} + l\cdot(\varepsilon_k + \varepsilon_{k+1})}. \quad (3)$$

j_o is the spherical Bessel function of zero order and S_k is the dielectric mismatch coefficient for the self-polarization. The direct Coulomb energy $\Delta E_c(a)$ arises when more than two electrons are put into the centred QD and interact with each other and is given by

$$\Delta E_c(a) = \frac{2.578}{\varepsilon_1 a}. \quad (4)$$

The induced polarization energy $\Delta E_p(a)$ depicts the interaction energy of the electron with the image charge created by another electron, expressed as

$$\Delta E_p(a) = \frac{e^2}{4\pi\varepsilon_o\varepsilon_1 a}\left[\sum_{\substack{k>0\\ k=\text{odd}}}^{n} \frac{1}{a}\cdot\frac{P_k}{1+((k-1)/2)(1+(b/a))} + \sum_{\substack{k>0\\ k=\text{even}}}^{n} \frac{1}{a}\frac{P_k}{(b/a)+((k-2)/2)(1+(b/a))} \right], \quad (5)$$

$$P_k = \frac{\varepsilon_k - \varepsilon_{k+1}}{\varepsilon_k\varepsilon_{k+1}}, \quad (6)$$

where P_k is the dielectric mismatch coefficient for the induced polarization. Both $\Delta E_s(a)$ and $\Delta E_p(a)$ are related to the b/a ratio, the parameter characterizing the multi-shell structure in the calculation. Hence, the concurrent effect on the blue shift $\Delta E_g(a)$ of the QD as illustrated in figure 2(*a*) can be ascribed to the size-dependent *quantum confinement energy* $\Delta E_g^{\text{Brus}}(a)$ and the *dielectric confinement energy* $\Delta E_g^{\text{dielectric}}(a)$ due to the dielectric mismatch. It can be expressed as [2–4,23,29]

$$\Delta E_g(a) = \Delta E_g^{\text{Brus}}(a) + \Delta E_g^{\text{dielectric}}(a) = \Delta E_g^{\text{Brus}}(a) + [2\Delta E_s(a) + \Delta E_c(a) + \Delta E_p(a)], \quad (7)$$

$$\Delta E_g^{\text{Brus}}(a) = \frac{\hbar^2\pi^2}{2a^2}\left[\frac{1}{m_e^*} + \frac{1}{m_h^*}\right] - \frac{1.8e^2}{\varepsilon_o\varepsilon_\infty a}. \quad (8)$$

$\Delta E_g^{\text{Brus}}(a)$ represents the quantum localization of the electron–hole via a shielded Coulomb interaction in a single QD, i.e. the ground-state regardless of the polarization in Brus' model [2, 19]. m_e^* and m_h^* are the effective masses of the electron and hole, respectively, and ε_∞ is the high-frequency dielectric constant of the QD. In our calculation, the quantum localization and the perturbation energy of the Coulomb interaction are both related to the wave functions of the electron and hole which can be characterized by the effective radius a_{eff} . Thus, we replace a by a_{eff} in equations (4) and (8). We note that the real dot radius a was adopted in equations (2) and (5) since the perturbation energies of the potential generated by the dielectric mismatch with the electron wave function are mainly constrained by the real dimension of the potential well, the effective radius a_{eff} can be obtained by applying the finite potential model with the following equation [31]

$$a_{\text{eff}} = a + \frac{\hbar}{\sqrt{2m_b^*(V_o - \Delta E_e(a))}}, \quad (9)$$

where V_o is the finite barrier potential, m_b^* is the effective mass of electron in the barrier region (SiO_2 matrix) and $\Delta E_e(a)$ is the electron confinement energy term in $\Delta E_g^{\text{Brus}}(a)$.

3.2. Confinement behaviours in various dielectric environments

To evaluate the confinement behaviour of a reality ZnO QDs/SiO_2 system, we designed three dielectric structures based on the multi-shell two-electron system model:

(1) structure 1: a single ZnO QD embedded in the SiO_2 matrix (figure 2(*b*));

Table 2. The parameters for the calculation of the dielectric confinement energy of QD in various dielectric structures.

	Structure 1	Structure 2	Structure 3
QD	ZnO	ZnO	ZnO
Dielectric environment	SiO_2 matrix	ZnO–SiO_2 composite matrix	ZnO/SiO_2 multishell
n	1	1	n [a]
b/a	∞	∞	
ε	$\varepsilon_1 = \varepsilon_{ZnO}\varepsilon_2 = \varepsilon_{SiO_2}$	$\varepsilon_1 = \varepsilon_{ZnO}\varepsilon_2 = \varepsilon^{(a)}_{matrix}$	$\varepsilon_1 = \varepsilon_3 = \varepsilon_5 = \ldots = \varepsilon_{ZnO}\varepsilon_2 = \varepsilon_4 = \varepsilon_6 = \ldots = \varepsilon_{SiO_2}$

[a] Listed in table 1.

Note: $\varepsilon_{ZnO} = 8.5$, $\varepsilon_\infty = 6$, $m_e^* = 0.3m_o$, $m_h^* = 0.8m_o$ [30]; $\varepsilon_{SiO_2} = 3.9$, $m_b^* = 0.5m_o$; $V_o = 4.3\,eV = \phi_{ZnO} - \phi_{SiO_2}$, ϕ = work function.

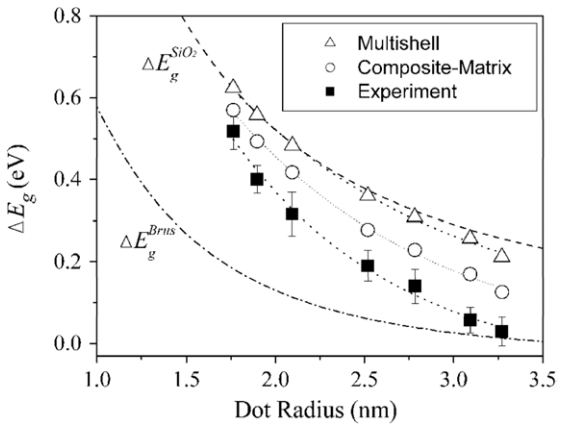

Figure 3. A comparison of experimental and calculated blue shifts ΔE_g of different dielectric structures based on the multi-shell two-electron system model.

(2) structure 2 (*composite matrix structure*): a single ZnO QD embedded in the composite ZnO–SiO_2 matrix (figure 2(*c*)) of which the dielectric constants ε_{matrix} are calculated by the Maxwell-Garnett approximation [32] with the ZnO volume ratio obtained from the measurement of x-ray reflectivity;
(3) structure 3 (*multi-shell structure*): a single ZnO QD embedded in the multi-shell dielectric environment comprising an alternative arrangement of SiO_2 and ZnO shell layers (figure 2(*d*)).

The parameters for the calculation are listed in tables 1 and 2. The calculation result and experimental data are presented in figure 3. The dashed–dotted line represents $\Delta E_g^{Brus}(a)$, the quantum localization derived by Brus without considering the effect of the outer dielectric environment. The uppermost dashed line represents $\Delta E_g^{SiO_2}(a)$, the dielectric confinement behaviour in structure 1, i.e. a single ZnO QD completely surrounded by the pure SiO_2 matrix. Figure 3 shows that the composite matrix structure (structure 2) and the multi-shell structure (structure 3) exhibit similar dielectric confinement tendencies. However, the multi-shell structure predicts larger blue shifts $\Delta E_g(a)$ and the values are almost superimposed with those of structure 1, especially for samples with a smaller dot radius and a larger b/a ratio. An analogous behaviour is observed in the experimental data as well. The figure reveals that the experimental blue shifts $\Delta E_g(a)$ are much smaller than those calculated by both the composite matrix structure and the multi-shell structure. As for samples with a larger dot radius and a small b/a ratio, they tend to have experimental $\Delta E_g(a)$ values closer to that predicted by Brus, indicating a weaker dielectric confinement.

Accordingly, we conclude that the composite matrix structure provides a better approximation of the blue shift $\Delta E_g(a)$ than the multi-shell structure, in spite of the difference between the calculation and the experiment result suggesting an inadequacy of the two-electron system. The reason is ascribed to the basic assumption of the two-electron system which takes into account only a single positively charged QD. The ground-state energy thereof is evaluated by considering the perturbations of the induced polarization potential on the energy of electrons in the single QD. In practice, each ZnO QD in the SiO_2 matrix behaves as an individual positive space charge. The dielectric confinement energy is affected by the neighbouring positive charges since the polarization potential induced by the charge accumulation is thus different. Moreover, figure 3 shows a larger deviation between the calculated and the experimental blue shifts $\Delta E_g(a)$ for samples with a large dot radius and a small b/a ratio. This leads us to believe in the existence of the weakening confinement without being considered in the two-electron system, such as the wave function tunnelling effect, which usually occurs between QDs when they are very close to one another [33–35].

3.3. The correlations of the dielectric confinement energy

In addition to the dielectric confinement effect described above, the experimental $\Delta E_g(a)$ can be further expressed in terms of $\Delta E_g^{Brus}(a)$:

$$\Delta E_g(a) = \Delta E_g^{Brus}(a) + \Delta E_g^{dielectric}(a) = \Delta E_g^{Brus}(a) + x \cdot \Delta E_{SiO_2}^{dielectric}(a), \quad (10)$$

where $\Delta E_{SiO_2}^{dielectric}(a)$ is the dielectric confinement energy of a single ZnO QD in the pure SiO_2 matrix (structure 1) and x is defined as the proportionality factor, representing the level of the similarity between the material system and structure 1. The proportionality factor x of each sample can be obtained through the calculation and the experiment result. Figure 4 shows the relations of the proportionality factor x versus the b/a ratio and ε_{matrix}. x increases linearly with the increase in the b/a ratio and declines with the increase in ε_{matrix}. It is quite apparent that when the b/a ratio increases, the system becomes more and more like structure 1 and the value of x becomes closer to unit. The increase in the b/a ratio represents the decrease in the total amount and density of ZnO QDs within the sample, implying that the value of ε_{matrix} gradually approaches the dielectric constant of the pure SiO_2 matrix. The correlation of the proportionality factor x with the b/a ratio and ε_{matrix} not only demonstrates the influence of the outer dielectric environment over the ground-state energy of QDs in nanocomposite thin films but also provides a simple method

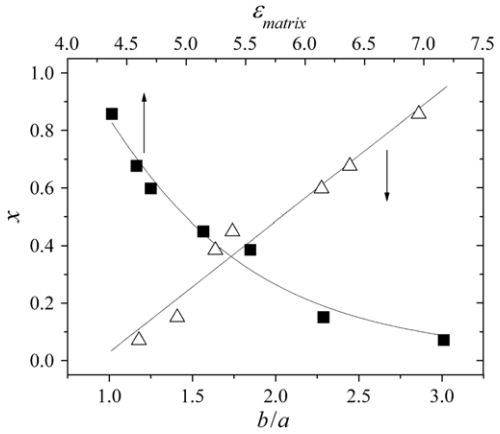

Figure 4. The relationships of the proportional factor x with the b/a ratio and the dielectric constant of the composite matrix $\varepsilon_{\text{matrix}}$. The curve fittings show a linear dependence of the proportionality factor x with the b/a ratio while a gradual decay with the dielectric constant of the composite matrix $\varepsilon_{\text{matrix}}$.

to evaluate the dielectric confinement effect in semiconductor QDs–dielectric systems.

4. Summary

In this work, we investigate the dielectric confinement effect on the blue shift ΔE_g of ZnO QDs embedded in the SiO_2 dielectric by applying the multi-shell two-electron system model. The blue shift ΔE_g of ZnO QDs with different dielectric structures is also calculated by considering the two-electron ground-state energy. In conjunction with the experimental data, we find that the composite matrix structure provides a better estimation of the blue shift ΔE_g of the ZnO QDs–SiO_2 system in comparison with the multi-shell structure. The relations of the proportionality factor x with the b/a ratio and the composite dielectric constant $\varepsilon_{\text{matrix}}$ indicate that the magnitude of the dielectric confinement energy depends on the similarity of the system with the structure containing only a single ZnO QD inside the pure SiO_2 matrix. The correlation of the calculation and the experimental result shows the modulability of electron energy states of ZnO QDs embedded in the dielectrics, which provides versatile engineering applications of the semiconductor QDs–dielectric systems in opto-electronic devices in the future.

Acknowledgments

This work is supported by the National Science Council (NSC) of the Republic of China under the contract of NSC95-2221-E-009-130. Y-Y P would like to acknowledge the NSC for the financial support given under the contract of NSC95-2112-M-213-005.

References

[1] Alivisatos A P 1996 *Science* **271** 933
[2] Brus L E 1983 *J. Chem. Phys.* **79** 5566
[3] Babić D, Tsu R and Grrne R F 1992 *Phys. Rev.* B **45** 14150
[4] Iwamatsu M, Fujiwara M, Happo N and Horii K 1997 *J. Phys.: Condens. Matter* **9** 9881
[5] Franceschetti A and Zunger A 2000 *Phys. Rev.* B **62** 2614
[6] Franceschetti A and Zunger A 2000 *Appl. Phys. Lett.* **76** 1731
[7] Orlandi A, Rontani M, Goldoni G, Manghi F and Molinari E 2001 *Phys. Rev.* B **63** 045310
[8] Bányai L, Gilliot P, Hu Y Z and Koch S W 1992 *Phys. Rev.* B **45** 14136
[9] Orlandi A, Goldoni G, Manghi F and Molinari E 2002 *Semicond. Sci. Technol.* **17** 1302
[10] Tkach N V and Fartushinski R B 2003 *Phys. Solid State* **45** 1347
[11] Bsiesy A, Muller F, Ligeon M, Gaspard F, Hérino R, Romestain R and Vial J C 1994 *Appl. Phys. Lett.* **65** 3371
[12] Linnros J, Lalic N, Kánpek P, Luterová K, Kočka J, Fejfar A and Pelant I 1996 *Appl. Phys. Lett.* **69** 833
[13] Collins R T, Fauchet P M and Tischler M A 1997 *Phys. Today* **50** 24
[14] Tsu R 1993 *Physica* B **189** 235
[15] Alperson B, Rubinstein I, Hodes G, Porath D and Millo O 1999 *Appl. Phys. Lett.* **75** 1751
[16] Banin U, Cao Y, Katz D and Millo O 1999 *Nature* **400** 542
[17] Cho C-H, Kim B-H, Kim T-W, Park S-J, Park N-M and Sung G-Y 2005 *Appl. Phys. Lett.* **86** 143107
[18] Efros Al L and Efros A L 1982 *Fiz. Tekh. Poluprovdn.* **16** 1209
[19] Brus L E 1984 *J. Chem. Phys.* **80** 4403
[20] Meirav U, Kastner M A and Wind S J 1990 *Phys. Rev. Lett.* **65** 771
[21] Yoshimura H, Schulman J N and Sakaki H 1990 *Phys. Rev. Lett.* **64** 22422
[22] Ye Q Y, Tsu R and Nicollian E H 1991 *Phys. Rev.* B **44** 1806
[23] Allan G, Delerue C, Lannoo M and Martin E 1995 *Phys. Rev.* B **52** 11982
[24] Peng Y Y, Hsieh T E and Hsu C H 2006 *Nanotechnology* **17** 174
[25] Peng Y Y, Hsieh T E and Hsu C H 2006 *Appl. Phys. Lett.* **89** 211909
[26] Fonoberov V A and Balandin A A 2004 *Phys. Rev.* B **70** 195410
[27] Viswanatha R, Sapra S, Satpati B, Satyam P V, Dev B N and Sarma D D 2004 *J. Mater. Chem.* **14** 661
[28] Böttcher J E 1973 *Theory of Electric Polarization* 2nd edn (Amsterdam: Elsevier)
[29] Das S, Chakrabarti S and Chaudhuri S 2005 *J. Phys. D: Appl. Phys.* **38** 4021
[30] Enright B and Fitzmaurice D 1996 *J. Phys. Chem.* **100** 1027
[31] Chuang S L 1995 *Physics of Optoelectronic Devices* (New York: Wiley) p 91
[32] Kingery W D, Bowen H K and Uhlmann D R 1991 *Introduction to Ceramics* (New York: Wiley)
[33] Na J H, Taylor R A, Rice J H, Robinson J W, Lee K H, Park Y S, Park C M and Kang T W 2005 *Appl. Phys. Lett.* **86** 083109
[34] Lee K H, Na J H, Taylor R A, Yi S N, Bimer S, Park Y S, Park C M and Kang T W 2006 *Appl. Phys. Lett.* **89** 023103
[35] Mazur Y I, Wang Z M, Tarasov G G, Xiao M, Salamo G J, Tomm J W and Talalaev V 2005 *Appl. Phys. Lett.* **86** 063102